

EXPERIMENTAL EVIDENCE FOR THE GRIFFITHS PHASE IN DISORDERED STRONGLY CORRELATED ELECTRON SYSTEMS: EXAMPLES*

ANDRZEJ ŚLEBARSKI 

Institute of Low Temperature and Structure Research, Polish Academy of Sciences
Okólna 2, 50-422 Wrocław, Poland
andrzej.slebarski@us.edu.pl

*Received 5 January 2026, accepted 30 January 2026,
published online 15 May 2026*

This report contributes to the ongoing discussion on the role of structural disorder and its impact on the physical properties of strongly correlated electron systems (SCESs). It has been theoretically predicted that, in the quantum critical regime, disorder arising from structural defects or doping can significantly influence the nature of the quantum macrostate in these materials. Disorder-driven mechanisms have also been proposed to explain the non-Fermi-liquid (NFL) behavior observed in such structurally disordered systems. The most prominent among these are the Kondo disorder scenario and an alternative model based on the Griffiths phase (GP). In this review, we extend these theoretical considerations through experimental investigations, providing empirical evidence for the existence of the GP state and/or Griffiths singularities in selected SCESs. Specifically, we examine the manifestation of the GP in CeRhSn with documented atomic disorder, Fe-doped $\text{Ce}_3\text{Co}_4\text{Sn}_{13}$ (Remeika phase), and selected Fe-based Heusler alloys.

DOI:10.5506/APhysPolB.57.5-A3

1. Introduction

Structural defects can significantly alter the physical properties of a system, particularly at low temperatures. Characterizing such defects using metallurgical techniques is not straightforward, especially when the defect is localized and/or occurs in small amounts. As a result, confirming the presence of a defect is typically based on indirect physical measurements that reveal new and unexpected phenomena.

* Presented at the Concepts in Strongly Correlated Quantum Matter Conference (CSCQM), Kraków, Poland, 20–22 November, 2025.

The effect of atomic disorder on the electronic properties of SCESs, particularly those close to a quantum critical point (QCP), has been the subject of research both experimental [1] and theoretical [2, 3]. It has been documented that these structural defects that act as perturbations could lead to substantial changes in the macrostate of the system. Disorder-driven mechanisms have been proposed, *e.g.*, to explain the non-Fermi-liquid (NFL) behavior of such structurally disordered systems. The most prominent among these are the Kondo disorder scenario [4–7] and an alternative model based on the Griffiths phase scenario [8–10]. Here, we present experimental evidence for the presence of the Griffiths phase in selected strongly correlated electron systems (SCESs).

The Griffiths phase is a state of matter that emerges in randomly disordered systems and lies between the magnetically ordered and paramagnetic phases, within the temperature range $T_C < T < T_G$. The concept was originally introduced for randomly diluted Ising ferromagnets [11]. The “classical” Griffiths phase is characterized by the presence of rare, large, non-interacting, and locally ordered regions (magnetic clusters) embedded in an otherwise disordered matrix. It manifests experimentally as a pronounced downturn in the inverse magnetic susceptibility, $\chi^{-1}(T)$. This breakdown of the smooth, analytical behavior in $\chi^{-1}(T)$ at the Griffiths temperature T_G is suppressed in the large magnetic field. Within a quantum Griffiths region (*i.e.*, below the crossover temperature T^* [10] for a disordered metallic Heisenberg anti-ferromagnet close to its quantum phase transition), the slow dynamics of rare regions give rise to the power-law singularities of χ electron specific-heat coefficient C/T and zero-temperature magnetization $M(H)$ [8, 10] ($\chi(T) \propto C/T(T) \propto T^{\lambda-1}$, $M \propto H^\lambda$, while magnetic susceptibility at low field obeys modified CW law, $\chi^{-1}(T) \propto (T - T_C^g)^{1-\lambda}$, where $0 < \lambda < 1$ is a Griffiths exponent and $T_C^g \gtrsim T_C$ is the critical temperature of random ferromagnetism where χ tends to diverge. Our current research focuses on strongly correlated *f*- and *d*-electron systems that contain various structural or substitutional defects and exhibit Griffiths phase-type behavior. To enhance structural disorder, our research is limited to polycrystalline systems. We present the characteristic behaviors of the Griffiths phase in both the “classical” and the “quantum” GP states observed for some selected compounds.

2. Experimental details

CeRhSn and the Remeika phases of $\text{Ce}_3\text{Co}_{3-x}\text{Fe}_x\text{Sn}_{13}$ were prepared by the arc melting technique and subsequent annealing at 800°C for 2 weeks. The samples were examined by X-ray diffraction (XRD) analysis (PANalytical Empyrean diffractometer equipped with a Cu $K\alpha_{1,2}$ source) and found to be a single-phase polycrystals with a structure, respectively: hexagonal

$P\bar{6}2m$ (CeRhSn) and cubic $Pm\bar{3}n$ ($\text{Ce}_3\text{Co}_{3-x}\text{Fe}_x\text{Sn}_{13}$, $x \leq 0.5$). The respective XRD patterns were analyzed with the Rietveld refinement method using the Fullprof Suite set of programs [12]. Details about the crystal structure of these compounds have previously been published [13–15]. Similarly, Fe-based Heusler alloys (L2₁-type cubic structure, symmetry $Fm\bar{3}m$) were obtained and analyzed (after the melting procedure, they were annealed for 2 weeks at 600°C, cf. [16]).

The stoichiometry and homogeneity of the samples were checked using an electron energy dispersive spectroscopy (EDS) technique. The atomic percentage of the specific element content in the obtained samples is close to the assumed composition with a deviation from the assumed composition at an acceptable level.

Magnetic measurements of dc were carried out in the temperature interval 1.8–400 K employing a superconducting quantum interference device (SQUID) magnetometer. The magnetic susceptibility of ac, $\chi_{ac} = \chi' + i\chi''$, was measured in the temperature range of 2 to 300 K using a Quantum Design Physical Property Measurement System (PPMS).

The heat capacity, C , was measured in the temperature range 0.5–300 K and in external magnetic fields of up to 9 T using the same PPMS platform.

The electrical resistivity, ρ , was investigated using a conventional four-point ac technique using a Quantum Design PPMS.

3. Evidence for Griffiths-Phase behavior revealed by magnetic measurements

3.1. Structurally disordered CeRhSn

CeRhSn is known as a paramagnetic heavy-fermion metal [13, 17], in which Ce ions are located in distorted kagome planes perpendicular to the c axis. However, when various local environments of the Ce atoms arising from local atomic disorder are taken into account, the *ab initio* calculations consistently yield a non-zero magnetic moment per formula unit ($\mu \neq 0$) [18], which, in turn, may explain the presence of dilute, non-interacting magnetic clusters, whereas the structurally ordered system is calculated to be paramagnetic. Moreover, recent investigations of magnetic properties at ultra-low temperatures did not rule out the possibility that geometrical frustration within the quasi-kagome ab plane drives CeRhSn into close proximity to a quantum critical point (QCP) [19–21]. In this regime, the system exhibits non-Fermi-liquid behavior [13], as evidenced by the power-law dependences $\chi \sim C/T \sim T^{-1+\lambda}$ and $M \sim H^\lambda$ observed between 2 and approximately 8 K, with $\lambda \cong 0.5$, characteristic of a quantum Griffiths phase (see Fig. 1). Figure 1(c) clearly shows a downturn in χ^{-1} at various applied magnetic fields around T_G . This downturn is significantly suppressed in high magnetic

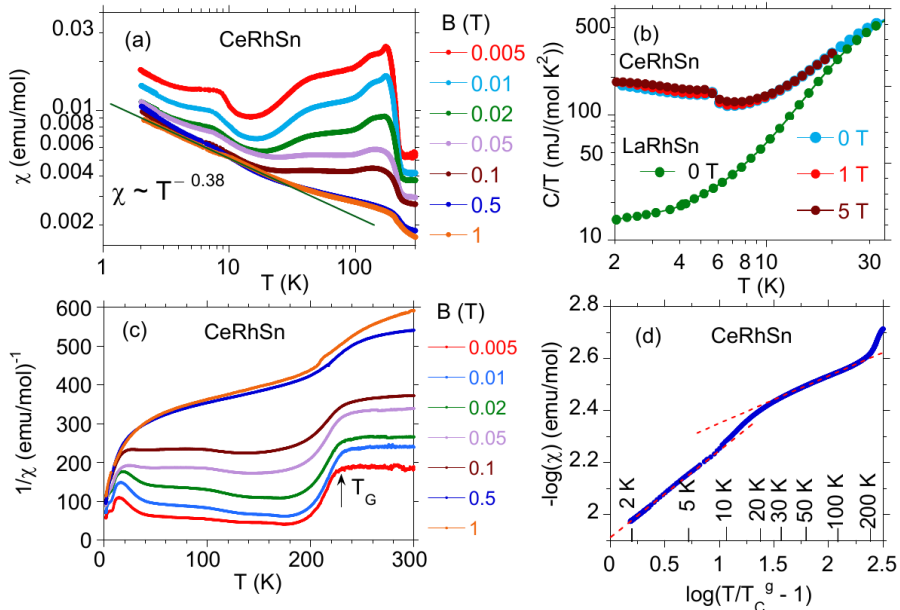


Fig. 1. CeRhSn: (a) The dc magnetic susceptibility $\chi(T)$ at different applied fields in log–log scale and $\chi \sim T^{-0.38}$ approximation. (b) The low-temperature $C(T)/T$ measured for CeRhSn at the field 0, 1, and 5 T in comparison with $C(T)/T$ obtained for LaRhSb at 0 magnetic field. (c) The inverse dc magnetic susceptibility $1/\chi(T)$ under different magnetic fields. (d) $1/\chi$ at $B = 0.5$ T versus $(T/T_C^g - 1)$ shown in log–log scale.

fields, supporting the presence of a GP in CeRhSn. The GP singularity follows the behavior of the power-law $\chi^{-1} \propto (T - T_C^g)^{1-\lambda}$, as illustrated in Fig. 1 (d). Two linear regions with different logarithmic slopes in $\log_{10}(\chi^{-1})$ indicate the presence of a classical GP state between T_G and approximately 25 K, separated from the quantum GP regime below about 8 K. In the intermediate temperature range, the GP coexists and interacts with a cluster-glass-like phase, complicating the interpretation (for details, see [14]).

Our modeling does not exclude the expected metamagnetic crossover observed in CeRhSn at the lowest temperatures (< 0.1 K) [19, 20], which excludes an itinerant scenario and suggests that frustration-induced quantum criticality is related to local moments in a liquid-like state of spin.

3.2. Griffiths phase in Heusler alloys

The Griffiths-phase behavior above the Curie temperature has been observed in a number of Heusler alloys. Of particular interest are alloys in which the coexistence of the GP and long-range disordered glassy magnetic

states emerges within the Griffiths region, thereby complicating a clear interpretation of the underlying physics (*cf.* [22]). Such behavior is often observed in Fe-based Heusler alloys.

Figure 2 shows the inverse susceptibility of dc $\chi^{-1} = B/M$ as a function of temperature for $\text{Fe}_2\text{VAI}_{1.35}$ in various applied magnetic fields. A Curie–Weiss (CW) law, $\chi \propto (T - \theta_{\text{CW}})^{-1}$, is obeyed for $T > 200$ K (see [16] for details). However, below the characteristic temperature $T_G \cong 200$ K, χ^{-1} displays a downward deviation from the CW law, indicating the onset of short-range ferromagnetic correlations. The $1/\chi$ *versus* T plots exhibit a clear downturn at T_G for $B < 50$ mT, along with a softening of the downward curvature and a pronounced field dependence associated with the magnetic-cluster-size effect. Upon further increasing B , the contribution from the paramagnetic matrix begins to dominate the GP response;

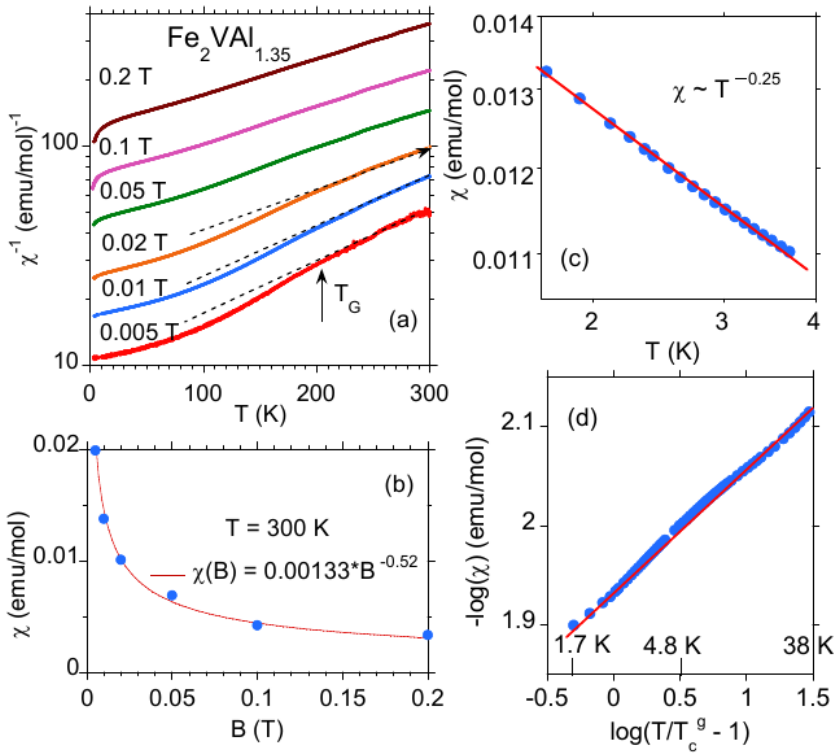


Fig. 2. Temperature dependence of inverse dc susceptibility χ^{-1} (in log scale) under different fields for $\text{Fe}_2\text{VAI}_{1.35}$. (b) χ (dc) obtained at 300 K *versus* applied magnetic field (blue points), and a power law fit to the data (red line). Inset (c) shows the divergent behavior of χ for $T < 4$ K, obtained at 0.1 T. Inset (d) presents $1/\chi$ *versus* reduced temperature ($B = 0.1$ T), $(T/T_G^g - 1)$ in the log–log scale.

ultimately, for $B > 100$ mT, the curve $\chi^{-1}(T)$ becomes nearly linear. All these features indicate a non-analytic behavior of M , which can be regarded a hallmark of the Griffiths singularity. For $T < 4$ K, χ exhibits a power-law behavior, $\chi \propto T^{-n}$, with the exponent $n = 1 - \lambda = 0.25$, as shown in Fig. 2(c). In the temperature range $1.7 < T < 40$ K, $\chi(T)$ can be well described by the expression $\chi(T) \sim (T - T_G^g)^{-(1-\lambda)}$ with the fitting parameters $T_G^g = 1.3$ K and $\lambda = 0.7$ (Fig. 2(d)). At $T = 2$ K, the magnetization follows the expected Griffiths-phase scaling, $M \propto B^\lambda$ [16]. It is worth noting that ac magnetic-susceptibility measurements additionally revealed signatures of a long-range, disordered, glassy magnetic state below $T \approx 15$ K $\ll T_G$ within the Griffiths-phase regime (not shown here; see Ref. [16]). This behavior appears to be rare, with a similar effect recently reported for Ni₂MnSb [22].

3.3. Cluster spin-glass-like behavior in the Griffiths regime of the “nonmagnetic” heavy-fermion filled-cage compound Ce₃Co₄Sn₁₃ doped with Fe

Finally, we show to what extent the systematic increase in disorder caused by Fe substitution can modify the effectiveness of the downward effect within the Griffiths-phase state. A good example appears to be the *non-magnetic quasiskutterudite compound* Ce₃Co₄Sn₁₃ (a Remeika-phase structure, $Pm\bar{3}n$) [23–25], doped with Fe [15], where the substitution level serves as a tunable disorder parameter. The small fraction of Ce atoms in the formula unit — three out of twenty atomic sites — leads the Fe-doped derivatives of Ce₃Co₄Sn₁₃ to be classified as diluted Kondo systems. Ce₃Co₄Sn₁₃ is a well-established heavy-fermion Kondo system that undergoes a crossover from a complex paramagnetic Kondo-lattice state — coexisting with weak magnetic correlations among diluted Ce moments [24, 25] — to a Kondo-impurity regime in magnetic fields of approximately 3 T [26]. This behavior suggests the proximity of the system to a quantum critical point (QCP) (*cf.* [27]). We find that even a modest substitution of Co with Fe ($x \approx 0.1$) leads to the formation of dilute, randomly distributed, and essentially non-interacting magnetic clusters, which becomes evident in the susceptibility $\chi(T)$ below $T_G \approx 200$ K. This results in a pronounced downward deviation from the Curie-like increase expected in the classical Griffiths-phase regime, as shown in Fig. 3(a)–(c). In addition, a field-induced enhancement of χ is observed upon reducing the applied magnetic field, similar to the behavior presented in Figs. 1 and 2 (the analogous field dependence for Ce₃Co_{3.5}Fe_{0.5}Sn₁₃ is not shown). Neither the downward deviation nor the field effect is observed when Fe is replaced by non-magnetic Ni dopants, as demonstrated in Fig. 3(d).

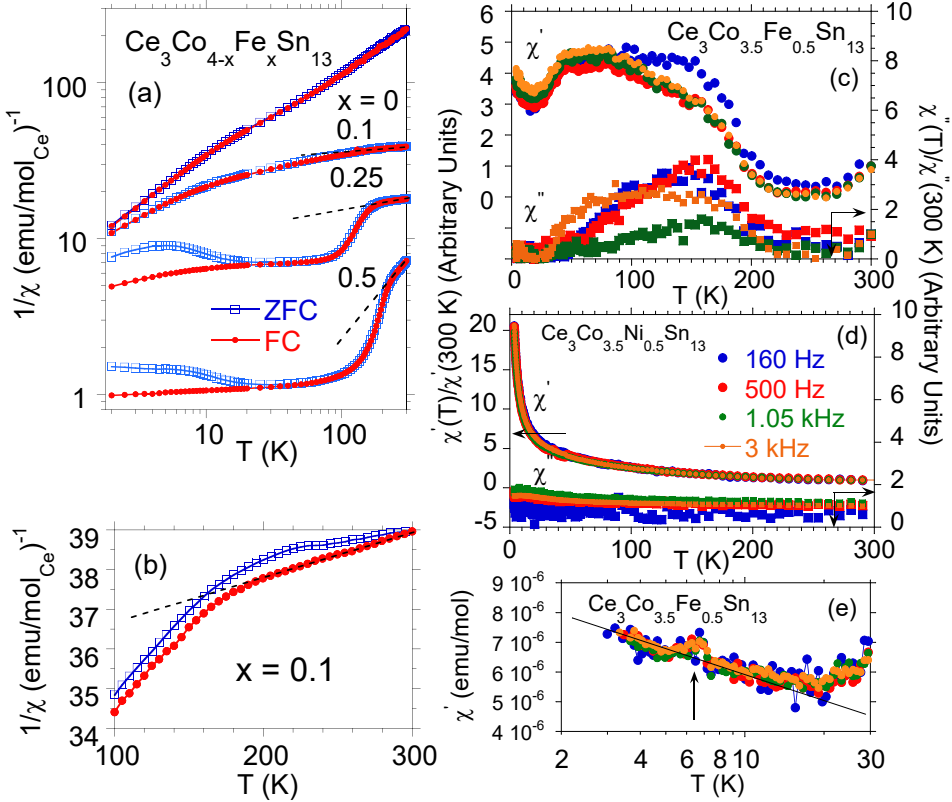


Fig. 3. (a) Evolution of the inverse dc susceptibility, $1/\chi(T)$ for $\text{Ce}_3\text{Co}_{4-x}\text{Fe}_x\text{Sn}_{13}$ at the field of 1000 Gs versus the content x of Fe dopant, shown in log–log scale in zero-field-cooled (ZFC) and field-cooled (FC) modes. (b) Details for sample $x = 0.1$ near $T_G \approx 180$ K. (c) The ac magnetic susceptibility $\chi_{ac}(T)$ versus temperature, measured for $\text{Ce}_3\text{Co}_{3.5}\text{Fe}_{0.5}\text{Sn}_{13}$ at different frequencies (ν) of the magnetic field with amplitude of 2 G. The maximal value of the component χ'' is $\sim 10^{-6}$ emu/g and its dependence on frequency ν can be negligible within an experimental error. (d) The comparison to the data for $\text{Ce}_3\text{Co}_{3.5}\text{Ni}_{0.5}\text{Sn}_{13}$ measured in identical physical conditions. (e) $\text{Ce}_3\text{Co}_{3.5}\text{Fe}_{0.5}\text{Sn}_{13}$; χ' versus T in log–log scales for $T < 30$ K [detail for panel (c)].

At lower temperatures, the ZFC–FC $\chi(T)$ bifurcation below ~ 20 K signals emerging cluster interactions and the onset of cluster-glass-like behavior within the Griffiths regime. This behavior strengthens with increasing Fe content and alters the $\chi \propto T^{-n}$ scaling. For $x = 0.1$, the power-law fit yields $n = 0.45$, while further Fe substitution reduces the exponent to $n = 0.26$

for $x = 0.25$ (in both ZFC and FC modes) and to $n = 0.06$ for $x = 0.5$ in the FC mode. Figure 3(e) shows the real component χ' of χ_{ac} for the $x = 0.5$ sample, which also follows the $\chi \propto T^{-n}$ behavior for $T < 10$ K. In addition, χ' displays a weak maximum near 6 K, indicative of magnetic inhomogeneity characteristic of a cluster-glass-like state.

Figure 4 shows magnetization isotherms M plotted as a function of B/T . For $4 < T < 20$ K, the M isotherms collapse onto a universal curve and exhibit no hysteresis, indicating superparamagnetic behavior below $T \approx 20$ K (*cf.* Fig. 3(a)). These $M(B/T)$ characteristics differ markedly from M versus B/T measured at 2 K, due to the exponential increase of the particle moment fluctuation time with decreasing temperature. As a result, M switches sharply to a more stable state below the blocking temperature of about 6 K, as seen in Fig. 3(e).

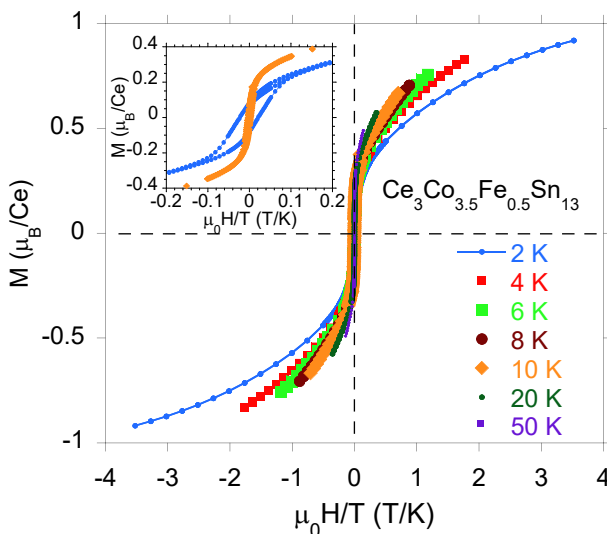


Fig. 4. $\text{Ce}_3\text{Co}_{3.5}\text{Fe}_{0.5}\text{Sn}_{13}$; Magnetization M versus $\mu_0 H/T$. The M isotherm at 2 K is approximated by the $M \propto (B/T)^\lambda$ (blue line), $\lambda = 0.39$. The inset shows M isotherms for $T = 2$ and 10 K in extended $\mu_0 H/T$ scale.

4. Concluding remarks

In summary, we have reviewed our experimental studies of the paramagnetic region of several selected SCES materials with atomic disorder, which exhibit Griffiths-phase behavior in the temperature range $T_C < T < T_G$, including quantum Griffiths singularities. A common feature of these materials is AS-type atomic disorder, which generates magnetic moments on atoms occupying AS positions. As a consequence, a classical Griffiths-phase state

emerges below a characteristic temperature T_G of about 200 K, accompanied by singular behavior in the low-temperature dc magnetic susceptibility, χ , and in the specific heat, C/T . The inverse dc magnetic susceptibility, $1/\chi$, plotted as a function of temperature, demonstrates that the classical Griffiths phase is sensitive to applied magnetic fields: as the field increases, the Griffiths-phase-related behavior gradually weakens and eventually disappears. The downward deviation from the Curie–Weiss law has been experimentally documented and discussed in CeRhSn, Fe-doped $\text{Ce}_3\text{Co}_4\text{Sn}_{13}$, and in the Heusler-type alloy $\text{Fe}_2\text{VAl}_{1+\delta}$ ($\delta \ll 1$). The choice of the materials studied here is not accidental: all of these systems are strongly correlated electron systems with documented Griffiths-phase behavior at similar characteristic temperatures, $T_G \sim 200$ K, as well as the onset of spin- or cluster-glass-like order in the low-temperature regime $T \ll T_G$. We investigated the effects of magnetic inhomogeneity interplaying with NFL-like behavior, as exemplified by CeRhSn, which can be systematically enhanced, for example, by Fe doping of the paramagnetic $\text{Ce}_3\text{Co}_4\text{Sn}_{13}$ Kondo-impurity system. Finally, cluster-glass-like long-range order emerging above T_C may coexist with the Griffiths phase, as recently documented for $\text{Fe}_2\text{VAl}_{1+\delta}$ [16]. For comparison, CeRhSn is a paramagnetic quasi-kagome Kondo lattice exhibiting quantum-critical behavior induced by geometrical frustration at ultralow temperatures [19], with a Griffiths phase forming below T_G [14].

Following Vojta [10], we attribute the diluted cluster-glass phase to the presence of rare regions, in which the slow dynamics of clusters can give rise to power-law singularities in many observables, such as the magnetic susceptibility χ , the electronic specific-heat coefficient C/T , and the zero-temperature magnetization $M(H)$. Within the Vojta model, the quantum Griffiths singularities can be observed in the temperature range $T_f < T < T^*$, where T_f is the cluster spin-freezing temperature due to RKKY interactions, and T^* denotes the crossover temperature separating the classical and quantum Griffiths phases. So, for CeRhSn, the characteristic temperature is $T^* \approx 9$ K, while for $\text{Ce}_3\text{Co}_{4-x}\text{Fe}_x\text{Sn}_{13}$ it is $T^* \approx 20$ K.

The dc magnetic susceptibility of $\text{Fe}_2\text{VAl}_{1+\delta}$ exhibits characteristic features commonly associated with a Griffiths phase below T_G . However, the interpretation of the $\chi(T)$ and $C(T)/T$ data for this alloy remains unclear in the low-temperature regime. $\text{Fe}_2\text{VAl}_{1+\delta}$ displays non-Fermi-liquid-like behavior, with the magnetic susceptibility following $\chi \propto T^{-0.25}$ for $T < 4$ K (*cf.* [16]), which has been interpreted as indicative of the possible formation of a quantum Griffiths phase. Nevertheless, similar behavior in $\chi(T)$ may also be attributed to Kondo effect associated with Fe antisite (AS) impurities [28]. If spin compensation were the dominant mechanism governing the low-temperature magnetic behavior, the susceptibility would instead be expected to follow a $T^{-0.5}$ dependence in the low-temperature limit [29], in

clear disagreement with the experimental observations. Therefore, in the case of this alloy, the interpretation of the low-temperature thermodynamic properties remains unclear.

REFERENCES

- [1] J.A. Mydosh, «Disorder and frustration in heavy-fermion compounds», *Physica B: Condens. Matter* **259–261**, 882 (1999).
- [2] J. Spałek, W. Wójcik, «A Strong Effect of Disorder on Mott Transition: Hubbard–Lloyd Model», *Acta Phys. Pol. B* **34**, 399 (2003).
- [3] C. Grenzbach, F.B. Anders, G. Czycholl, T. Pruschke, «Influence of disorder on the transport properties of heavy-fermion systems», *Phys. Rev. B* **77**, 115125 (2008).
- [4] V. Dobrosavljević, T.R. Kirkpatrick, G. Kotliar, «Kondo Effect in Disordered Systems», *Phys. Rev. Lett.* **69**, 1113 (1992).
- [5] E Miranda, V Dobrosavljević, G Kotliar, «Kondo disorder: a possible route towards non-Fermi-liquid behaviour», *J. Phys.: Condens. Matter* **8**, 9871 (1996).
- [6] E. Miranda, V. Dobrosavljević, G. Kotliar, «Disorder-Driven Non-Fermi-Liquid Behavior in Kondo Alloys», *Phys. Rev. Lett.* **78**, 290 (1997).
- [7] O.O. Bernal, D.E. MacLaughlin, H.G. Lukefahr, B. Andracka, «Copper NMR and Thermodynamics of $\text{UCu}_{5-x}\text{Pd}_x$: Evidence for Kondo Disorder», *Phys. Rev. Lett.* **75**, 2023 (1995).
- [8] A.H. Castro Neto, G. Castilla, B.A. Jones, «Non-Fermi Liquid Behavior and Griffiths Phase in f -Electron Compounds», *Phys. Rev. Lett.* **81**, 3531 (1998).
- [9] A.H. Castro Neto, B.A. Jones, «Non-Fermi-liquid behavior in U and Ce alloys: Criticality, disorder, dissipation, and Griffiths–McCoy singularities», *Phys. Rev. B* **62**, 14975 (2000).
- [10] T. Vojta, «Quantum Griffiths Effects and Smeared Phase Transitions in Metals: Theory and Experiment», *J. Low Temp. Phys.* **161**, 299 (2010).
- [11] R.B. Griffiths, «Nonanalytic Behavior Above the Critical Point in a Random Ising Ferromagnet», *Phys. Rev. Lett.* **23**, 17 (1969).
- [12] J. Rodriguez-Carvajal, «Recent advances in magnetic structure determination by neutron powder diffraction», *Physica B: Condens. Matter* **192**, 55 (1993).
- [13] A. Ślebarski *et al.*, «Strongly correlated electron behaviour in the compound CeRhSn », *Phil. Mag. B* **82**, 943 (2002).
- [14] A. Ślebarski, M.M. Maška, «Griffiths phases in structurally disorder CeRhSn : Experimental evidence and theoretical modeling», *Phys. Rev. B* **111**, 235106 (2025).
- [15] L. Kalinowski, M. Kądziołka-Gaweł, A. Ślebarski, «Cluster spin-glass behavior in heavy-fermion-filled cage $\text{Ce}_3\text{Co}_4\text{Sn}_{13}$ doped with Fe: Magnetic and Mössbauer effect studies», *Phys. Rev. B* **98**, 245140 (2018).

- [16] A. Ślebarski *et al.*, «Off-stoichiometric effect on magnetic and electron transport properties of $\text{Fe}_2\text{VAl}_{1.35}$ and Ni_2VAl : A comparative study», *Phys. Rev. B* **109**, 165105 (2024).
- [17] M.S. Kim *et al.*, «Low-temperature anomalies in magnetic, transport, and thermal properties of single-crystal CeRhSn with valence fluctuations», *Phys. Rev. B* **68**, 054416 (2003).
- [18] A. Ślebarski, A. Jezierski, «Non-Fermi liquid behavior in CeRhSn coexistent with magnetic order», *Phys. Stat. Sol. B* **236**, 340 (2003).
- [19] Y. Tokiwa *et al.*, «Characteristic signatures of quantum criticality driven by geometrical frustration», *Sci. Adv.* **1**, e1500001 (2015).
- [20] S. Kittaka *et al.*, «Field-Angle-Resolved Landscape of Non-Fermi-Liquid Behavior in the Quasi-Kagome Kondo Lattice CeRhSn », *J. Phys. Soc. Jpn.* **90**, 064703 (2021).
- [21] S. Kimura *et al.*, «Anisotropic non-Fermi liquid and dynamical Planckian scaling of a quasi-kagome Kondo lattice system», *npj Quantum Mater.* **10**, 85 (2025).
- [22] F. Tian *et al.*, «Griffiths phase arising from local lattice distortion and spin glass above the Curie temperature in Ni_2MnSb polycrystalline Heusler alloy», *Phys. Rev. B* **109**, 224405 (2024).
- [23] J.P. Remeika *et al.*, «A new family of ternary intermetallic superconducting/magnetic stannides», *Solid State Commun.* **34**, 923 (1980); J.L. Hodeau, M. Marezio, J.P. Remeika, C.H. Chen, «Structural distortion in the primitive cubic phase of the superconducting/magnetic ternary rare-earth rhodium stannides», *Solid State Commun.* **42**, 97 (1982).
- [24] E.L. Thomas *et al.*, «Crystal growth, transport, and magnetic properties of $\text{Ln}_3\text{Co}_4\text{Sn}_{13}$ ($\text{Ln} = \text{La}, \text{Ce}$) with a perovskite-like structure», *J. Solid State Chem.* **179**, 1642 (2006).
- [25] A.L. Cornelius *et al.*, «Observation of field-induced single impurity behavior in the heavy fermion compound $\text{Ce}_3\text{Co}_4\text{Sn}_{13}$ », *Physica B: Condens. Matter* **378–380**, 113 (2006).
- [26] $\text{Ce}_3\text{Co}_4\text{Sn}_{13}$ does not show any sign of long-range magnetic ordering down to 0.35 K [25]. It, however, exhibits a short-range antiferromagnetic order at 0.8 K, which can be suppressed by magnetic field, giving way to single-impurity behaviour above ~ 3 T with a Kondo temperature $T_K \approx 1.2$ K [25].
- [27] A. Ślebarski, J. Goraus, «Field-induced phase transition in $\text{Ce}_3\text{M}_4\text{Sn}_{13}$ with $\text{M} = \text{Co}, \text{Rh},$ and Ru », *Physica B: Condens. Matter* **536**, 165 (2018).
- [28] The magnetoresistance (MR) isotherms of $\text{Fe}_2\text{VAl}_{1+\delta}$ can be collapsed onto a single curve when plotted as a function of $B/(T + T_K^*)$, where T_K^* is a characteristic temperature [16]. Schlottmann-type scaling [30] applied to this Heusler alloy yields $T_K^* = 2.9$ K, supporting the presence of the Kondo effect in this material.
- [29] P.W. Anderson, «Ground State of a Magnetic Impurity in a Metal», *Phys. Rev.* **164**, 352 (1967).
- [30] P. Schlottmann, «Bethe-Ansatz solution of the ground-state of the $\text{SU}(2j + 1)$ Kondo (Coqblin–Schrieffer) model: Magnetization, magnetoresistance and universality», *Z. Phys. B* **51**, 223 (1983).